02MSEC-15

An Angle of Attack Correction Scheme for the Design of Low Aspect Ratio Wings with Endplates

Michael Soso and Michael S. Selig
University of Illinois at Urbana-Champaign

ABSTRACT

Low aspect ratio wings are used extensively on open-wheeled race cars to generate aerodynamic downforce. Consequently, a great deal of effort is invested in obtaining wing profiles that provide high values of lift coefficient. If the wings are designed using 2-D methods, then it is necessary to take into account the change in operating angle of a typical airfoil section that occurs when it operates in the downwash generated by the wing. Accounting for this change during the design phase will ensure that the airfoil sections are optimized for their intended operating conditions. The addition of endplates to the wing serves to counteract the magnitude of the change in operating angle by effectively producing an increase in wing aspect ratio.

During the design process at UIUC, an empirical method was used to provide an estimate of the effective aspect ratio of the wing and endplate combination. However, owing to concerns about the dependence of the formula on the chord of the endplate beyond the chord of the wing, it was decided to attempt to develop a new effective aspect ratio relation. Using CFD, a study was carried out to investigate the aerodynamic changes that occurred when a low aspect ratio wing was used in conjunction with endplates of varying height and varying chord. The angle of attack of the wing was also changed in the study. The aerodynamic changes were then used to deduce changes in the effective aspect ratio.

The resulting data showed that the effective aspect ratio was highly dependent on an increase in the height of the endplate and slightly dependent on changes in the wing angle of attack. There was no significant dependence on the chord of the endplate beyond the chord of the wing. These results were then used to develop a formula linking the aspect ratio of the wing to the effective aspect ratio of the wing/endplate combination

INTRODUCTION

BACKGROUND - The field of aerodynamics is one of the major areas of research and development in modern motorsports, a consequence of the fact that many different avenues that can be exploited in order to effect continuous improvement to the race cars [1, 2]. Possibly the most intensely researched area centers around the generation of maximum downforce on the cars. Downforce is needed on race cars because it enhances the performance envelope of the vehicle by providing an increase in its lateral acceleration and braking capabilities [3–5]. Ultimately, the performance gain leads to a reduction in lap times as the vehicle becomes more competitive. The wings on a race car generate the majority of the available downforce, therefore a great deal of attention is given to the proper design and analysis of these components.

At UIUC, the tool used for race car wing design is PROFOIL/MFOIL [6]. It is a 2-D multipoint inverse design method that allows for the specification of a required velocity distribution or boundary layer development in order to produce a candidate airfoil that satisfies the design requirements. Wing design is therefore carried out in 2-D even though the actual situation is 3-D based. Consequently, concerns arise as to whether the 3-D effects can be adequately accounted for in the initial design phase. In making the 2-D to 3-D transition, the airfoil, a wing of infinite span, now becomes a wing of finite span. The tips of the wing become regions where the flow from the bottom of the wing mixes with the flow from the top, eventually forming two large streamwise vortices. These vortices induce a downward velocity behind the wing, which in conjunction with the freestream velocity, form a resultant velocity about the wing. The direction of the resultant velocity differs from that of the freestream velocity, and as a consequence, the lift vector produced by the wing is tilted backwards by an angular amount known as the induced angle of attack. The induced angle of attack has the effect of reducing the effective local freestream angle of attack, which now becomes less than that of the original airfoil in 2-D. The addition of endplates to the wing serves to counteract the magnitude of the angular reduction. Consequently during the design process, the extent of the angular reduction has to be accounted for, or the wing will be designed for a higher operating point that is actually necessary.

ENDPLATES - The ability of endplates to improve the performance of wings has been widely established. Early theoretical work [7, 8], aimed mainly at induced drag reduction, showed that the load per unit span of a wing was dependent on the height of the endplate and that the circulation was dependent on the ratio of the height of the endplate to the span of the wing. Figure 1 provides a comparison of the lift distribution of a typical wing with and without the presence of endplates. The results were obtained from a CFD evaluation using Fluent 5 commercial CFD package. There is a clear increase in the lift per unit span of the wing with the addition of the endplates. The result can effectively be considered as an increase in the aspect ratio of the wing, since a wing of the same profile but greater aspect ratio may be able to provide the same lift distribution as that obtained by the addition of endplates.

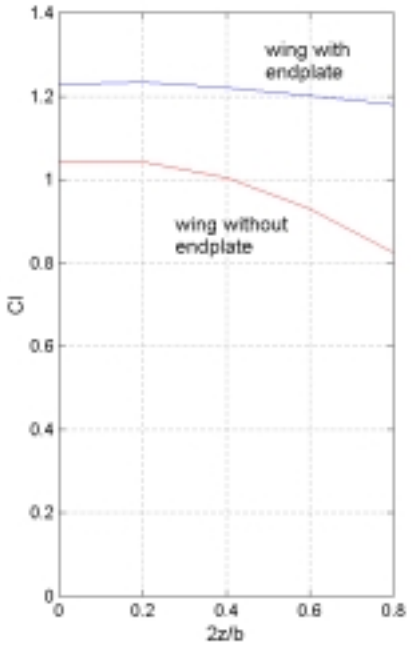

Figure 1: The lift distribution of a wing without an endplate and with the presence of an endplate. The results were obtained by performing a comparative CFD analysis in Fluent 5.

Reports on experimental work concerning the estimation of the effective aspect ratio of wings with endplates can be found in Refs. [9-12]. More specifically, Hoerner [11] and Schlichting and Truckenbrodt [12], presented a general formula linking the physical characteristics of wings with endplates to their aerodynamic characteristics. Hoerner's correlation was dependent on the ratio of the endplate height to wing span (*h*/*b*) and a constant k = 1.9. His formulation, given in Eq. 1, is valid for (*h*/*b*) up to 0.4. He also stated that excess endplate area beyond the chord of the attached wing did not significantly contribute to the effective aspect ratio.

$$AR_{eff} = AR\left[1+1.9\left(\frac{h}{b}\right)\right] \qquad (1)$$

Schlichting's and Truckenbrodt's correlation, Eq. 2, which incidentally was used in the design process at UIUC, differed from the previous equation in that it was dependent on ratios of the chord of the wing to the dimensions of the endplate. Here b_V is the endplate height, c_V is the endplate chord and c_H is the wing chord. It also allowed the effective aspect ratio to increase with increasing endplate chord beyond the chord of the wing, in contrast to Hoerner's results. The resulting discrepancy provided the impetus to develop an effective aspect ratio correlation for wing design at UIUC.

$$AR_{eff} = AR\left[1+\frac{1}{2}\frac{b_V}{c_V}\left(\frac{c_V}{c_H}\right)^2\right] \qquad (2)$$

UIUC DESIGN - A brief overview of the UIUC airfoil design method as previously given in Ref. [13] will be outlined, since it has direct bearing on the way in which the effective aspect ratio was finally determined in this study. Figure 2 shows a 2-D profile of a 3-D wing and endplate along with velocity vectors for a typical race car situation, except that the airplane convention is used in that the wing is lifting. The freestream velocity V_∞ is parallel to the top and bottom edges of the endplate. Note that in the figure, the induced angle of attack is referenced with respect to the freestream and not the chord line. Since the wing is of finite span it produces a downwash. Following the approach taken by McCormick [14] for high lift wings, this downwash is taken as perpendicular to the local velocity vector V_L, which differs from the classic approach of being perpendicular to the freestream.

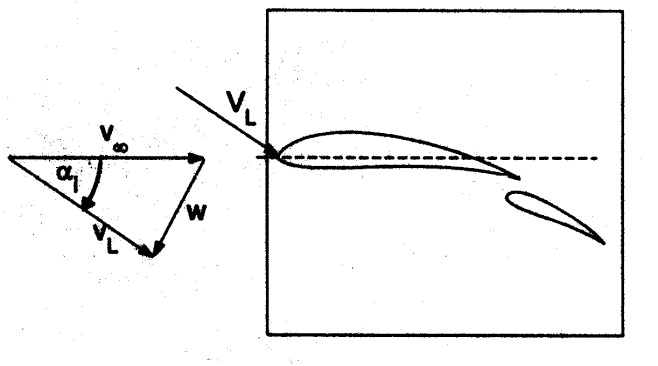

Figure 2: A diagram used for the development outlined in Ref. [13].

Using this diagram along with the lift and drag forces developed by the wing, it is possible to derive Eq. 3 [13], which when plotted with the 2-D lift curve of the airfoil section, gives an estimate of the operating point of the section. Figure 3 shows the resulting plot, and highlights the fact that the operating point depends on the estimated value of the effective aspect ratio.

$$C_l = \pi AR_{eff}\tan(\alpha_i) \qquad (3)$$

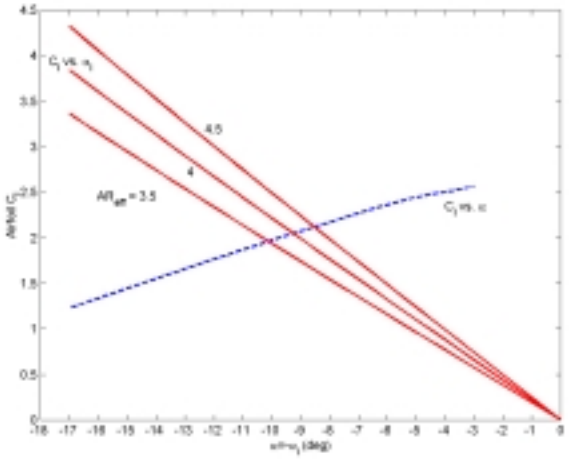

Figure 3: The determination of the predicted operating point for a typical airfoil, where the operating point is the intersection of the 2-D lift curve of the airfoil and Eq. 3.

METHODOLOGY

COMPUTATIONAL GEOMETRY - The current study entailed a variation in the aspect ratio of the endplate at a constant wing angle of attack, along with a variation in the angle of attack of the wing at constant endplate aspect ratio. The wing used in the study was derived from the UIUC700 two-element airfoil [15, 16]. It consisted of an untwisted rectangular wing having a chord of 0.32 m and a span of 0.925 m, yielding a geometric aspect ratio of 2.88. Figure 4 presents the geometry used in the first part of the investigation. Three main trade studies were carried out in order to quantify independently the effects of angle of attack, endplate height and endplate chord. In each case, the flap was set to 21 deg relative to the chord of the main plane. In Fig. 4, the baseline geometry is denoted as 5degM, corresponding to a 5 deg angle of attack with medium width endplate chord. In the first trade study, the endplate height was increased by a maximum of 40% relative to the baseline. For the second study, the endplate chord was increased in the upstream direction by a maximum of 61.7%. For the third study, the angle of attack was set at 1, 5, and 9 deg, designated as 1degM, 5degM and 9degM respectively (not depicted in Fig. 4). The angle of attack was changed via a rotation about the leading edge of the main plane.

All cases were modelled with CFD software from Fluent Inc., Lebenon NH. The geometry and mesh were created in the preprocessor Gambit, while the solution was obtained with the use of Fluent 5. The hardware used in the study consisted of the Origin system of supercomputers at the National Center for Supercomputing Applications (NCSA). Figure 5 shows the geometry in the computational domain. The domain was constructed with a velocity inlet boundary condition 20 chords ahead of the wing and a pressure outlet condition at least 25 chords behind the wing. This ensured that the boundary conditions at infinity did not influence the flow conditions in the immediate vicinity of the wing. Symmetry boundary conditions were used at the centerline of the computational domain to mirror the second half of the model and on the outer side of the domain, located 10 chords from the origin. The resulting cell count was 1,630,000. The Reynolds number based on wing chord was 1.45e6, which allowed for the use of the RNG κ-ε model with non-equilibrium wall functions.

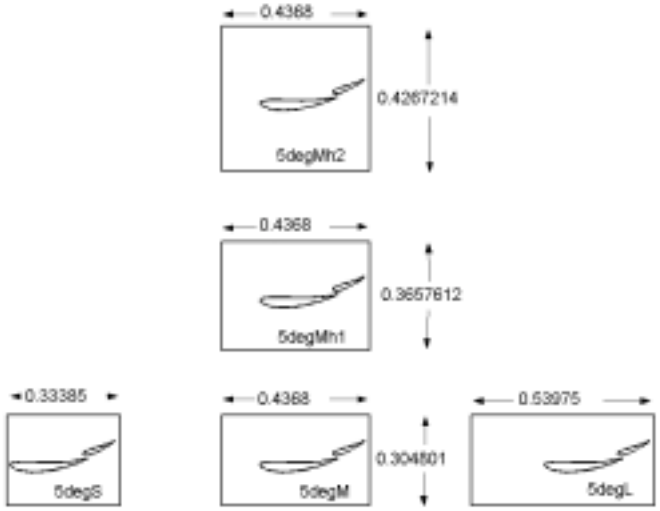

Figure 4: Geometries used in the aspect ratio study at 5 deg.

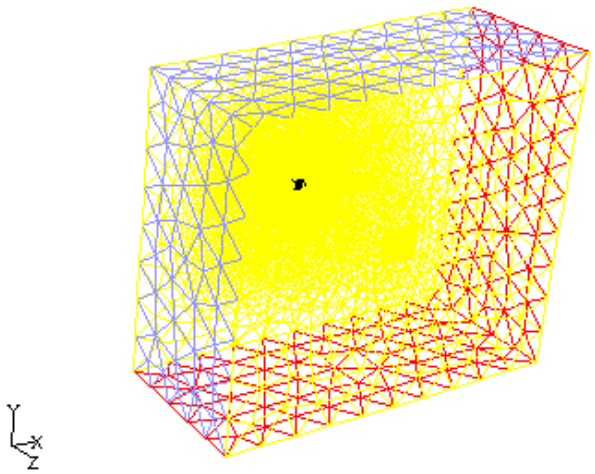

Figure 5: The computational domain used in the study.

EFFECTIVE ASPECT RATIO – The objective of the research was to obtain an estimate of the effective aspect ratio for each wing/endplate configuration. In order to achieve this goal, the intent was to use the tools previously developed (the C_l vs. α_i and the C_l vs. α plots), but to reverse the order of the procedure. If the operating point of the airfoil section at the wing centerline were known in terms of its lift coefficient, then it would be possible to use the information to determine the effective aspect ratio by using the two plots of Fig. 3.

An iterative procedure was used to determine the effective aspect ratio. To this end, Fig. 6 illustrates the

variables and conventions used in the process. *N'* is the normal force per unit span and is perpendicular to the chord of the wing. *L'* is the lift per unit span and is perpendicular to the local velocity vector V_L. The geometric angle of attack of the wing is α_g. Also shown are α_i, the induced angle of attack, and α, the local angle of attack relative to the chordline. The iterative procedure used to find the effective aspect ratio and the equations used in its development are outlined as follows:

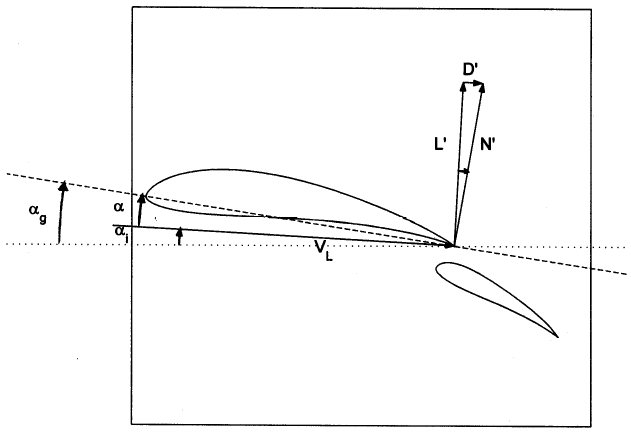

Figure 6: the velocity vector diagram used to obtain the angular relations in the determination of the effective aspect ratio.

1. A guess was made for AR_{eff}, α and V_L. V_L was then used to obtain C_n in the next step.

2. Referencing Fig. 6, it can be deduced that

$$C_n = \frac{N'}{\frac{1}{2}\rho V_L^2 c} \quad (4)$$

   with *N'* being obtained from Fluent post-processing.

3. C_n and α were then used to obtain C_l with the use of $C_l = C_n \cos \alpha$..

4. With the calculated C_l value, a new estimate of α was obtained from the 2-D lift curve of the airfoil section.

5. The C_l value was also used in the following equation to obtain an estimate of the downwash.

$$w = V_\infty \arcsin\left(\frac{C_l}{\pi AR_{eff}}\right) \quad (5)$$

6. The downwash estimate was then used to obtain a new estimate of the local velocity in

$$V_L = \sqrt{V_\infty^2 - w^2} \quad (6)$$

7. A new estimate of α_i was then determined from $\alpha_i = \alpha_g - \alpha$..

8. C_l and α_i were then substituted into Eq.3 to obtain an updated estimate of AR_{eff}. The newly computed α, V_L, and AR_{eff} were then used in step 2, and the process was repeated until convergence was achieved; the result of which is AR_{eff}.

RESULTS

DATA ANALYSIS - Table 1 presents two sets of effective aspect ratio results. AR_{eff_SS} was computed from the iterative procedure previously outlined. AR_{eff_ST} was obtained from Eq. 2 as previously given. A comparison of the results showed that there was an increase in the effective aspect ratio as the height of the endplate was increased. Figure 7 presents the data as a bar graph. It can be deduced that AR_{eff_ST} predicted much higher values of effective aspect ratio than did AR_{eff_SS}. The change in effective aspect ratio was also much greater for AR_{eff_ST}. Considering endplate M as the baseline case, endplate Mh2 produced a 15.7% increase in AR_{eff_ST} in comparison to a 7.29% increase in AR_{eff_SS}.

Table 1: Variation of effective aspect ratio with increasing endplate height. Endplate M is the shortest, while endplate Mh2 is the tallest.

Configuration	AR_{eff_SS}	AR_{eff_ST}
5degM	3.98	4.77
5degMh1	4.12	5.14
5degMh2	4.27	5.52

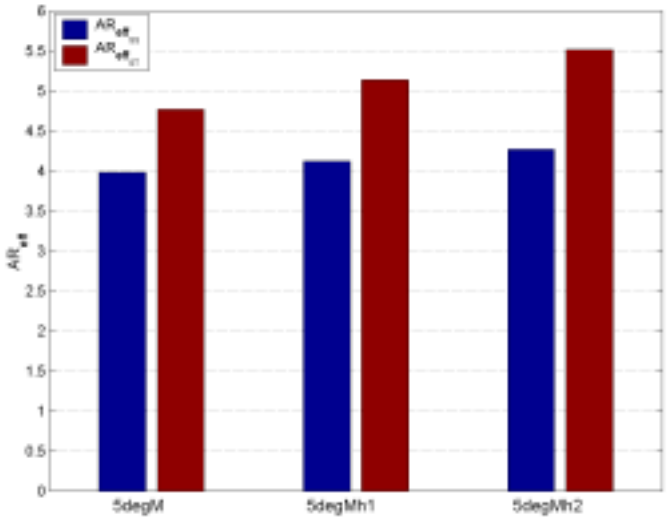

Figure 7: A comparison of AR_{eff_SS} and AR_{eff_ST} while increasing the height of the endplate.

Table 2 presents the effective aspect ratio results obtained from increasing the chord of the endplate beyond the chord of the wing. A plot of the data is given in Fig. 8. Inspection showed that AR_{eff_ST} predicted a significant increase in the effective aspect ratio, while AR_{eff_SS} hardly predicted any increase. As compared with endplate S, endplate L showed and increase of 20.6% for AR_{eff_ST}, in comparison to 1.27% for AR_{eff_SS}. AR_{eff_SS} followed the trend indicated by Hoerner [11]. He stated that excess area beyond the chord of the attached wing did not significantly contribute to the effective aspect ratio.

Table 2: Variation of effective aspect ratio with increasing endplate chord.

Configuration	AR_{eff_SS}	AR_{eff_ST}
5degS	3.94	4.32
5degM	3.98	4.77
5degL	3.99	5.21

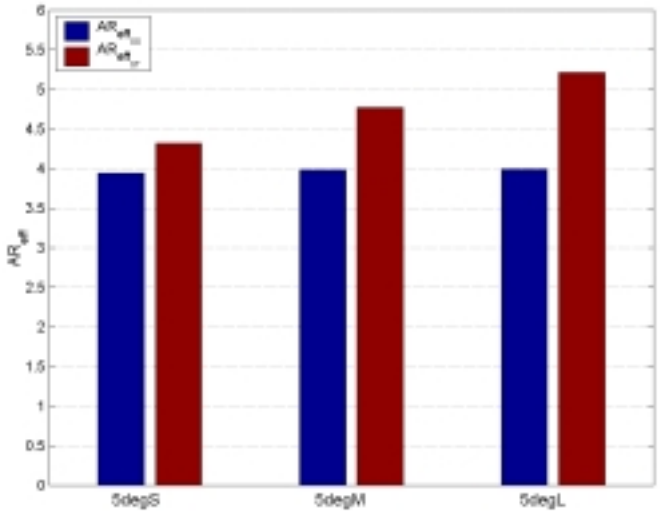

Figure 8: A comparison of AR_{eff_SS} and AR_{eff_ST} while increasing the chord of the endplate beyond the chord of the wing.

Table 3 presents the effective aspect ratio results obtained while increasing the angle of attack of the wing. Endplate M was common to the three cases. Inspection of the table and Fig. 9 showed that AR_{eff_SS} predicted a slight increase (2.82%) in the effective aspect ratio when compared to AR_{eff_ST}, which predicted no increase. Since the effective aspect ratio depends on geometric factors, the change predicted by AR_{eff_SS} was unexpected, and will be the subject of future investigation.

Table 3: Variation of the effective aspect ratio while increasing the wing angle of attack.

Configuration	AR_{eff_SS}	AR_{eff_ST}
1degM	3.90	4.77
5degM	3.98	4.77
9degM	4.01	4.77

.

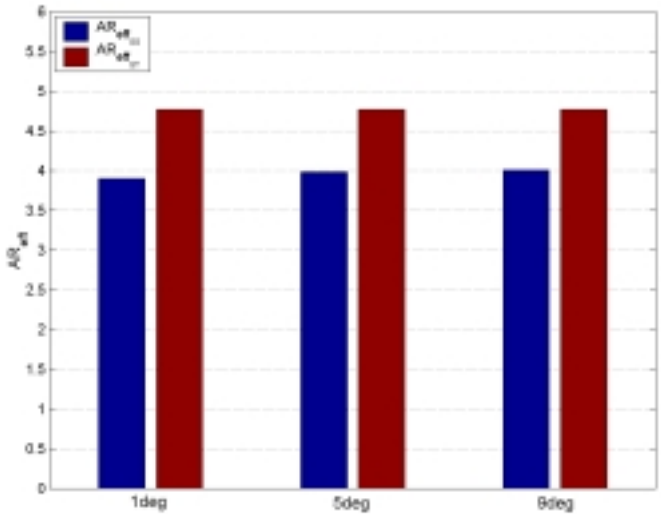

Figure 9: A comparison of AR_{eff_SS} and AR_{eff_ST} while increasing the wing angle of attack.

EFFECTIVE ASPECT RATIO FORMULA - An approach that can be use to develop an effective aspect ratio formula will now be discussed. The idea, which was derived from a method discussed in Ref. [17], will be to use a constant *k* to link the effective aspect ratio of the wing/endplate combination with the aspect ratio of the wing in isolation through the equation given by

$$AR_{eff} = k(AR) \tag{8}$$

The constant *k* can be tabulated for the factors that influence the effective aspect ratio. In this case, the factors were the change in height of the endplate, the change in the chord of the endplate and the change in the wing angle of attack. As the previously depicted, the effective aspect ratio was dependent on a change in the height of the endplate and a change in the freestream angle of attack. Therefore, two separate constants can be tabulated to represent each of the effects.

Figure 10 presents a plot of k_h, while increasing the height of the endplate. The endplate height is represented by *h*, while *c* represents the chord of the wing and not the chord of the endplate. The chord of the wing was used because it can be considered as being the limiting factor, after analyzing the effective aspect ratio results obtained from increasing the chord of the

endplate. Referring to Fig. 4, it can be deduced that it would be misleading to normalize by the chord of the endplate, since increasing this variable beyond the chord of the wing did not produce a significant change in effective aspect ratio. Figure 11 presents a plot of k_{ang} with increasing freestream angle of attack. A polynomial curve has been fit through the points.

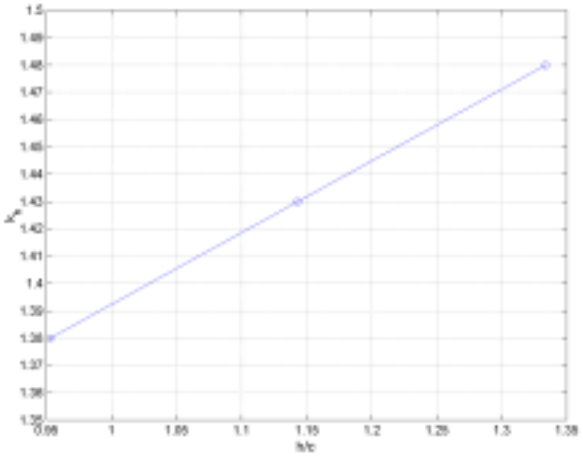

Figure 10: A plot of the constant k_h versus the ratio of the height of the endplate to the chord of the wing, (h/c).

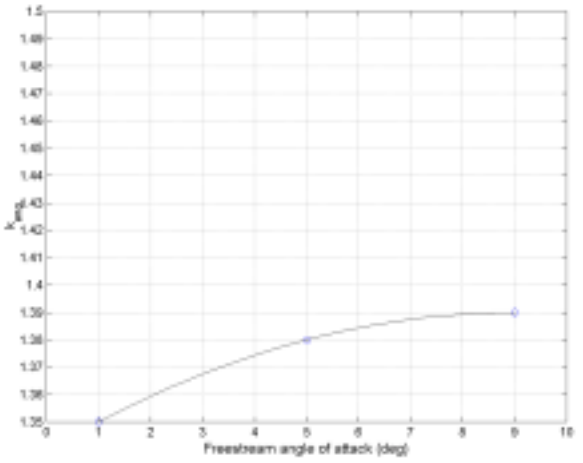

Figure 11: A plot of the constant k_{ang} versus the freestream angle of attack.

CONCLUSION

A method for the determination of the effective aspect ratio of a low aspect ratio wing with endplates was developed by finding the operating point of an airfoil section at the centerline of the wing. The results showed that the most significant variable affecting the effective aspect ratio was a change in the height of the endplate. Increasing the endplate height by 40% produced an effective aspect ratio increase of 7.29%.

Increasing the chord of the endplate, which was already greater than the chord of the wing, produced a very slight change in effective aspect ratio. The chord was increased by 61.7% and produced a corresponding increase of 1.27% in the effective aspect ratio.

Increasing the angle of attack of the wing, while keeping the endplate geometry fixed, unexpectedly produced an effective aspect ratio change. A change in angle of attack of 8 deg produced a 2.82% increase in effective aspect ratio. Since the effective aspect ratio should not be dependent on angle of attack, this result will be the subject of future investigation.

REFERENCES

1. Wright, P. G., “The Influence of Aerodynamics on the Design of Formula One racing cars,” International Journal of Vehicle Design, Vol. 3, 1982, pp 383–397.
2. Dominy, J. A., and Dominy, R. G., “Aerodynamic influences on the performance of the Grand Prix racing car,” Proc Instn Mech Engrs, Vol. 198D, 1984, pp 87–93.
3. Adams, H., “Chassis Engineering,” HPBooks, Los Angeles, CA, 1993.
4. Gillespie, T. D., “Fundamentals of Vehicle Dynamics," SAE, Inc., Warrendale, PA, 1992.
5. Wright, P. G., “Formula 1 Technology,” SAE, Inc., Warrendale, PA, 2001.
6. Gopalarathnam, A., and Selig, M. S., “Design of High-Lift Airfoils for Low Aspect Ratio Wings with Endplates,” AIAA Paper 97-2232, June 1997.
7. Von Karman, Th., and Burgers, J. M., “General Aerodynamic Theory - Perfect Fluids. Airfoils and Airfoil Systems of Finite Span,” Vol. 2, Aerodynamic Theory, E 4, Section 19, W. F. Durand, ed., Julius Springer (Berlin), 1935, pp 211–212.
8. Mangler, W., “The Lift Distribution of Wings with End Plates,” NACA TM No. 856. Translated from “Die Auftriebsverteilung am Tragflugel mit Endscheiben,” Luftfahrtforschung, Vol. 14, No. 11, November 20, 1937, pp. 564–569.
9. Reid, E. G., “The Effects of Shielding the Tips of Airfoils,” NACA Technical Report No. 201, 1925.
10. Riley, D. R., “Wind-Tunnel Investigation and Analysis of the Effects of End Plates on the Aerodynamic Characteristics of an Unswept Wing,” NACA TN 2440, June 1951.
11. Hoerner, S. F., “Fluid Dynamic Drag,” Hoerner Fluid Dynamics, 1965.
12. Schlichting, H., and Truckenbrodt, E., “Aerodynamics of the Airplane,” McGraw-Hill Inc., 1979, pp 441–442.
13. Gopalarathnam, A., and Selig, M. S., “Design of High-Lift Airfoils for Low Aspect Ratio Wings with Endplates,” AIAA Paper 97-2232, June 1997.
14. McCormick, Jr., B. W., “`Aerodynamics of V/STOL Flight,” Dover Publications Inc., 1967, pp 51–65.
15. Jasinski, W.J. and Selig, M.S, “Experimental Study of Open-Wheel Race-Car Front Wings,” SAE 1998

Transactions - Journal of Passenger Cars,Vol. 107, Section 6, 1999.
16. Jasinski, W.J. and Selig, M.S, “Experimental Study of Open-Wheel Race-Car Front Wings," SAE Motorsports Engineering Conference and Exposition, SAE Paper No 983042, Dearborn, MI, November 1998.
17. Aird, Forbes, “Aerodynamics for Racing and Performance Cars,” HPBooks, June 1997, pp 98–99.